HHS Public Access

Author manuscript

Science. Author manuscript; available in PMC 2017 July 31.

Published in final edited form as:

Science. 2016 September 09; 353(6304): 1147–1151. doi:10.1126/science.aag0822.

Spatiotemporal microbial evolution on antibiotic landscapes

Michael Baym[1], **Tami D. Lieberman**[1,†], **Eric D. Kelsic**[1], **Remy Chait**[1,‡], **Rotem Gross**[2], **Idan Yelin**[2], and **Roy Kishony**[1,2,3,*]

[1]Department of Systems Biology, Harvard Medical School, Boston, MA USA

[2]Faculty of Biology, Technion – Israel Institute of Technology, Haifa, Israel

[3]Faculty of Computer Science, Technion – Israel Institute of Technology, Haifa, Israel

Abstract

A key aspect of bacterial survival is the ability to evolve while migrating across spatially varying environmental challenges. Laboratory experiments, however, often study evolution in well-mixed systems. Here we introduce an experimental device, the Microbial Evolution and Growth Arena (MEGA) plate, in which bacteria spread and evolve on a large antibiotic landscape (120x60cm), allowing visual observation of mutation and selection in a migrating bacterial front. While resistance increases consistently, multiple coexisting lineages diversify both phenotypically and genotypically. Analyzing mutants at and behind the propagating front, we find that evolution is not always led by the most resistant mutants; highly resistant mutants may be trapped behind more sensitive lineages. The MEGA-plate provides a versatile platform for studying microbial adaption and a direct seeing-is-believing visualization of evolutionary dynamics.

Main Text

The worldwide increase in antibiotic resistance has motivated numerous studies aimed at understanding the phenotypic and genotypic evolution of antibiotic resistance (1–7). These experiments have shed light on the tradeoffs constraining adaptive evolution in single and multi-drug environments (5, 6, 8, 9). However, most of our current knowledge about the evolution of resistance is based on laboratory setups with well-mixed environments (1–7, 10, 11).

In natural and clinical settings, bacteria migrate between spatially distinct regions of selection (5, 6, 8, 9, 12, 13). Theoretical models show that spatially structured pressures change the nature of selection: instead of competing with its neighbors for limited resources, an adapted individual needs only be the first capable of venturing and surviving in a new

*Corresponding author. roy_kishony@hms.harvard.edu.
†Current address: MIT, Cambridge, MA, USA
‡Current address: IST Austria, Klosterneuburg, Austria

Supplemental Materials
Materials and Methods
Figures S1 to S6
Tables S1 and S2
Movies S1 to S5
References 35–41

region (14, 15). A pioneering study, focusing on small population sizes, showed that structured microenvironments increase the rate of adaptation to antibiotics through highly reproducible genetic changes (16). It is unknown how evolution is shaped by the diversification potential and differences in adaptive constraints of large populations in spatial environments.

Here, we present a device for the evolution of bacteria that allows migration and adaptation in a large, spatially structured environment. The Microbial Evolution and Growth Arena (MEGA) plate consists of a rectangular acrylic dish (120 x 60 cm) in which successive regions of black-colored agar containing different concentrations of antibiotics are overlaid by soft agar allowing bacterial motility (Fig. 1A). Motile bacteria inoculated at one location on the plate deplete nutrients locally and then spread by chemotaxis to other regions (17). Only increasingly resistant mutants can spread into sections containing higher levels of antibiotic. The large size of the plate serves two purposes: it provides for a large population and mutational supply, and it maintains the antibiotic gradient despite diffusion (since drug diffusion time scales quadratically with distance while the bacterial front advances linearly, the large plate size prevents the antibiotic gradient from equilibrating over the duration of the experiment). Critically, once a mutant has exhausted the resources of a region of the plate, other mutants do not significantly chemotax to that region (since, without a nutrient gradient, they move diffusively). In this manner, mutational lineages can block each other physically, a phenomenon notably observed in biofilm formation (18). This partitioning of mutants into stable spatial domains also enables sampling of individual mutants for later analysis. Using periodic photography of the plate we constructed time-lapse movies of evolution (movie S1). Combining these with analysis of isolates, this system allows reconstruction of the phenotypic and genotypic evolutionary histories of evolving bacteria.

Challenging bacteria in spatial gradients of antibiotics leads to large increases in resistance through sequential adaptive steps across competing lineages (Fig. 1; movie S1). We first set up the MEGA-plate with symmetric four-step gradients of trimethoprim (TMP) or ciprofloxacin (CPR) proceeding inwards with tenfold increases in concentration per step (Fig. 1A, TMP: 0, 3, 30, 300, 3000x wild-type Minimum Inhibitory Concentration, MIC; CPR: 0, 20, 200, 2000, 20000x MIC) and inoculated the drug free regions with *Escherichia coli*. Bacteria swim and spread until they reach a concentration in which they can no longer grow (TMP: Fig. 1C and movies S1 and S2; CPR: movie S3). As resistant mutants arise in the population, their descendants migrate into the next step of drug concentration and fan out (Fig. 1C, 88h). Adjacent mutant lineages exclude each other and compete for limited space, resulting in some lineages entirely blocking off growth of others (Fig. 1C). When the winning lineages reach a further increased level of drug concentration at which they, too, are unable to grow, secondary mutations arise, and the process repeats. Ultimately, the bacteria reach and overspread the highest drug concentration, showing dramatic increases in drug resistance (phenotyping sampled mutants from the highest concentration region showed 10,000-fold increase in MIC for TMP, Fig. 1B; 100,000-fold increase for CPR, fig. S1). The adaption time (10 days in TMP; 12 days in CPR) is consistent with evolution in well mixed environments (4), yet is slower than reported adaptation rates in micro-spatial environments, likely a result of the additional time required to swim between concentration steps (9). It is possible that at different dimensions the MEGA-plate will yield different evolutionary

dynamics; a wider front would increase the effective population size and thus the mutational supply, while a longer run between steps would increase selection among adjacent lineages.

To test the importance of the size of intermediate steps in the evolution of high-level resistance, we set up a variant of the MEGA-plate in which bacteria go from no drug to a high level directly or through one middle region of variable magnitude (Fig. 2. TMP: high step 3000; middle step 0, 3, 30, or 300 MIC. CPR: high step 2000; middle step 0, 2, 20, or 200 MIC). Bacteria were unable to adapt directly from zero to the highest concentration of either drug. Diffusive smoothing of these large steps enabled the appearance of partially resistant mutants, but their lineages did not advance (Fig. 2A, left). The addition of an intermediate concentration step enabled adaptation, although this was impeded when this middle step was too high (Fig. 2B). Even across the permissive intermediate steps, evolution often proceeded through multiple mutations taking advantage of the local gradients formed by diffusion (TMP: movie S4, CPR: movie S5). Thus, by progressing through colonization of regions with moderately challenging selective pressures, intermediate-resistance mutants can expand to sufficient numbers to facilitate the rise of high-resistance mutants. Analogous to evolutionary rescue in temporal selective gradients (19–21), a gradual spatial gradient allows adaptation to previously inhospitable environments. Unlike in a temporal gradient, though, a spatial gradient does not impose a minimal time for a mutant's appearance and spread; at any time, a mutant appearing on the stalled front can expand and evolve further, provided it is sufficiently resistant to colonize the next step. Thus, concordant with theoretical predictions (22, 23), access to intermediate regions of moderate selection is critical for enabling a range of evolutionary paths to high-level resistance.

We next focused on the genotypic and phenotypic paths leading to high levels of resistance. We sequenced 21 isolates from the four-step TMP gradient experiment and 230 isolates from the multiple intermediate-step TMP experiment above. Samples separated into minimally and highly mutated, i.e. mutator phenotype, groups (>60 single nucleotide polymorphisms [SNPs] and indels for high; <12 for low; Fig. 3A). Similar separation was also seen when restricting the analysis to synonymous mutations to minimize differential effects of selection (fig. S2). All highly mutated isolates, but none of the others, had mutations in *dnaQ* (also called *mutD*), which was the only gene for which the presence of a mutation correlated perfectly with the mutator phenotype. This gene encodes DNA polymerase III which is critical to proofreading (22, 23). Isolates carrying mutated *dnaQ* alleles showed increased rates of mutations on rifampin disk diffusion assays (fig. S2)(24). These mutators appeared repeatedly in distinct locations on the plate and across experiments. Based on lineage reconstructions from the time-lapse video as well as genotypic relationships, the mutator phenotype emerged at least six times independently between the four-step and intermediate-step TMP experiments above (fig. S2; four different alleles of *dnaQ* were observed: V96E, I97N, I97S, I97T, where I97T appeared three independent times). While these mutator lineages accumulated mutations more rapidly, their rate of phenotypic adaption was similar to that of the less mutated isolates (reaching the highest level of resistance at roughly the same time, fig. S3 and movie S4). Indeed, the highly mutated lineages had a close to neutral ratio of non-synonymous to synonymous substitutions (Fig. 3B). In contrast, the less mutated isolates showed a high bias towards coding mutations, indicating that most of these mutations were likely adaptive (Fig. 3B).

Focusing on the non-mutator isolates, we identified a wide spectrum of putatively adaptive mutations for trimethoprim resistance. The most frequently mutated gene was the primary target of trimethoprim, *folA* (25), which encodes dihydrofolate reductase (DHFR) (Fig. 3C), with more mutations appearing as resistance increased. We also observed several genes that were repeatedly mutated yet are not involved in the folate biosynthesis pathway, and thus not primarily associated with trimethoprim resistance. These included stress response genes, such as those of the *mar* and *sox* operons, known to be important in general antibiotic and toxin resistance (26), as well as genes involved in transcription and translation, which have been shown to affect trimethoprim resistance (27). We also found that three genes not classically associated with trimethoprim resistance were repeatedly mutated, often with a probable loss of function (frameshift or nonsense): a phosphate transporter (*pitA*), shikimate kinase I (*aroK*), and a negative regulator of the PhoQP system (*mgrB*). Knockout of these genes in the ancestral strain confirmed their resistance phenotypes (fig. S4).

Mutations that increased resistance often came with a cost of reduced growth, which was subsequently restored by additional, compensatory, mutations (28–30). While some resistance-conferring mutations allowed colonization of high drug concentration regions without affecting growth, many lineages capable of growing in the high drug regions were deficient in yield, particularly during CPR resistance evolution (as measured by optical density, Fig. 4A–B, for CPR; fig. S3 for TMP). These yield deficient mutations were followed by compensatory mutations allowing growth to full density (Fig. 4A,B; movie S3; number of compensatory mutants observed in a single run: >50 for TMP and >500 for CPR). In the absence of a chemotaxis-inducing nutrient gradient, the compensatory mutants stayed localized behind the front – appearing in a characteristic pattern of localized spots spreading from single points (movie S3; Fig. 4A).

Focusing on evolution in CPR, we sampled and phenotyped compensatory mutants, finding that many had not only compensated for growth but had also increased in resistance, often beyond the resistance levels of the propagating front (Fig. 4C). Yet, as these mutants were engulfed by their parental lineage, they stayed constrained to the immediate vicinity in which they appeared and were unable to overtake the moving front. To test whether these compensatory mutants were capable of outcompeting the propagating front, in an additional evolution experiment we sampled the trapped compensatory mutants and moved them forward, re-inoculating them ahead of the still-moving front. These compensatory mutants were able to grow in a region where the front could not (Fig. 4D). Similarly, some trapped compensatory mutants were able to outcompete their parent when placed side-by-side on a fresh gradient plate (fig. S5). Hence, as compensatory mutations often occur behind the front, they are spatially restricted from contributing to the ultimate evolutionary course of the population. Indeed, in the rare cases when these compensatory mutations appeared at the front, and were not physically blocked, they accelerated the adaptive process (movie S3, 00:53; fig. S3). Thus, the fitness of the population is not driven by the fittest mutants, but rather by those that are both sufficiently fit and arise sufficiently close to the advancing front.

While the MEGA-plate is not intended to directly simulate natural or clinical settings, it captures unique aspects of evolution during range expansion. Evolution of high levels of

resistance is enabled by intermediate regions of moderate selective pressure. Furthermore, as multiple lineages evolve in parallel, the propagating front can be led by lineages less fit than those trapped behind it.. It will be interesting to explore how adaptation rates and mutational diversity depend on other spatio-temporal parameters, including population density, mutation rate, and the relative expansion speed and spatial dimensions. Owing to the relaxed evolutionary constraints in range-expansion dynamics, the MEGA-plate is likely to reveal novel mutational pathways to high-level multi-antibiotic resistance. Further, the MEGA-plate can be adapted to a range of organisms and challenges beyond antibiotics. Importantly, differences in evolutionary dynamics between evolution under different selection pressures appear visually, simplifying both hypothesis generation and testing. Owing to this flexibility, the MEGA-plate is a platform for exploring the interplay of spatial constraints and evolutionary pressures. The MEGA-plate provides a physical analog of the otherwise abstract Muller plots of population genetics (31, 32) and of other elusive aspects of evolution, including diversification, compensatory mutations, and clonal interference. Its relative simplicity and ability to visually demonstrate evolution makes the MEGA-plate a useful tool for science education and outreach.

Supplementary Material

Refer to Web version on PubMed Central for supplementary material.

Acknowledgments

Sequence data is available on NCBI SRA under accession number SRP077287. We thank Xiaoyan Robert Bao, and Adam C. Palmer for helpful discussions. We thank the National BioResource Project (NIG, Japan) for providing the Keio collection. EDK acknowledges government support under and awarded by the Department of Defense, Office of Naval Research, National Defense Science and Engineering Graduate (NDSEG) Fellowship, 32 CFR 168a. This work was supported by a US National Institutes of Health grant R01-GM081617 (RK) and the European Research Council FP7 ERC Grant 281891 (RK).

References and Notes

1. Weinreich DM, Delaney NF, DePristo MA, Hartl DL. Darwinian Evolution Can Follow Only Very Few Mutational Paths to Fitter Proteins. Science. 2006; 312:111–114. [PubMed: 16601193]
2. Lee HH, Molla MN, Cantor CR, Collins JJ. Bacterial charity work leads to population-wide resistance. Nature. 2010; 467:82–85. [PubMed: 20811456]
3. Lane PG, Hutter A, Oliver SG, Butler PR. Selection of Microbial Mutants Tolerant To Extreme Environmental Stress Using Continuous Culture-Control Design. Biotechnol Prog. 1999; 15:1115–1124. [PubMed: 10585198]
4. Toprak E, et al. Evolutionary paths to antibiotic resistance under dynamically sustained drug selection. Nat Genet. 2012; 44:101–105.
5. Imamovic L, Sommer MOA. Use of collateral sensitivity networks to design drug cycling protocols that avoid resistance development. Sci Transl Med. 2013; 5:204ra132.
6. Lázár V, et al. Bacterial evolution of antibiotic hypersensitivity. Molecular Systems Biology. 2013; 9:700–700. [PubMed: 24169403]
7. Fridman O, Goldberg A, Ronin I, Shoresh N, Balaban NQ. Optimization of lag time underlies antibiotic tolerance in evolved bacterial populations. Nature. 2014; 513:418–421. [PubMed: 25043002]
8. Hegreness M, Shoresh N, Damian D, Hartl D, Kishony R. Accelerated evolution of resistance in multidrug environments. Proc Natl Acad Sci USA. 2008; 105:13977–13981. [PubMed: 18779569]

9. Zhang Q, et al. Acceleration of Emergence of Bacterial Antibiotic Resistance in Connected Microenvironments. Science. 2011; 333:1764–1767. [PubMed: 21940899]
10. Conrad TM, Lewis NE, Palsson BO. Microbial laboratory evolution in the era of genome-scale science. Molecular Systems Biology. 2011; 7:509–509. [PubMed: 21734648]
11. Kawecki TJ, Lenski RE, Ebert D, Hollis B. Experimental evolution. Trends in Ecology and Evolution. 2012; 27:547–560. [PubMed: 22819306]
12. Martínez JL. The role of natural environments in the evolution of resistance traits in pathogenic bacteria. Proc R Soc B. 2009; 276:2521–2530.
13. Hallatschek O, Hersen P, Ramanathan S, Nelson DR. Genetic Drift at Expanding Frontiers Promotes Gene Segregation. Proc Natl Acad Sci USA. 2007; 104:19926–19930. [PubMed: 18056799]
14. Greulich P, Waclaw B, Allen RJ. Mutational pathway determines whether drug gradients accelerate evolution of drug-resistant cells. Physical review letters. 2012; 109:088101. [PubMed: 23002776]
15. Hermsen R, Deris JB, Hwa T. On the rapidity of antibiotic resistance evolution facilitated by a concentration gradient. Proc Natl Acad Sci USA. 2012; 109:10775–10780. [PubMed: 22711808]
16. Zhang Q, et al. Acceleration of emergence of bacterial antibiotic resistance in connected microenvironments. Science. 2011; 333:1764–1767. [PubMed: 21940899]
17. Berg HC, Brown DA. Chemotaxis in Escherichia coli analysed by three-dimensional tracking. Nature. 1972; 239:500–504. [PubMed: 4563019]
18. Xavier JB, Foster KR. Cooperation and conflict in microbial biofilms. Proc Natl Acad Sci USA. 2007; 104:876–881. [PubMed: 17210916]
19. Bell G, Gonzalez A. Adaptation and Evolutionary Rescue in Metapopulations Experiencing Environmental Deterioration. Science. 2011; 332:1327–1330. [PubMed: 21659606]
20. Gonzalez A, Bell G. Evolutionary rescue and adaptation to abrupt environmental change depends upon the history of stress. Philosophical Transactions of the Royal Society of London B: Biological Sciences. 2013; 368:20120079–20120079. [PubMed: 23209161]
21. Lindsey HA, Gallie J, Taylor S, Kerr B. Evolutionary rescue from extinction is contingent on a lower rate of environmental change. Nature. 2013; 494:463–467. [PubMed: 23395960]
22. Fowler RG, Degnen GE, Cox EC. Mutational specificity of a conditional Escherichia coli mutator, mutD5. Molec Gen Genet. 1974; 133:179–191. [PubMed: 4614067]
23. Echols H, Lu C, Burgers PM. Mutator strains of Escherichia coli, mutD and dnaQ, with defective exonucleolytic editing by DNA polymerase III holoenzyme. Proc Natl Acad Sci USA. 1983; 80:2189–2192. [PubMed: 6340117]
24. Galán JC, et al. Fosfomycin and rifampin disk diffusion tests for detection of Escherichia coli mutator strains. J Clin Microbiol. 2004; 42:4310–4312. [PubMed: 15365030]
25. Smith DR, Calvo JM. Nucleotide sequence of dihydrofolate reductase genes from trimethoprim-resistant mutants of Escherichia coli. Evidence that dihydrofolate reductase interacts with another essential gene product. Mol Gen Genet. 1982; 187:72–78. [PubMed: 6761546]
26. Martin RG, Jair KW, Wolf RE, Rosner JL. Autoactivation of the marRAB multiple antibiotic resistance operon by the MarA transcriptional activator in Escherichia coli. J Bacteriol. 1996; 178:2216–2223. [PubMed: 8636021]
27. Bollenbach T, Quan S, Chait R, Kishony R. Nonoptimal microbial response to antibiotics underlies suppressive drug interactions. Cell. 2009; 139:707–718. [PubMed: 19914165]
28. Lenski RE. Bacterial evolution and the cost of antibiotic resistance. Int Microbiol. 1998; 1:265–270. [PubMed: 10943373]
29. Levin BR, Perrot V, Walker N. Compensatory mutations, antibiotic resistance and the population genetics of adaptive evolution in bacteria. Genetics. 2000; 154:985–997. [PubMed: 10757748]
30. Handel A, Regoes RR, Antia R. The role of compensatory mutations in the emergence of drug resistance. PLoS Comput Biol. 2006; 2:e137. [PubMed: 17040124]
31. Muller HJ. Some Genetic Aspects of Sex. The American Naturalist. 1932; 66:118–138.
32. Barrick JE, Lenski RE. Genome dynamics during experimental evolution. Nat Rev Genet. 2013; 14:827–839. [PubMed: 24166031]

33. Keseler IM, et al. EcoCyc: fusing model organism databases with systems biology. Nucleic Acids Research. 2012; 41:D605–D612. [PubMed: 23143106]
34. Baba T, et al. Construction of Escherichia coli K-12 in-frame, single-gene knockout mutants: the Keio collection. Molecular Systems Biology. 2006; 2 2006.0008.
35. Baym M, et al. Inexpensive multiplexed library preparation for megabase-sized genomes. PLoS ONE. 2015; 10:e0128036. [PubMed: 26000737]
36. Joshi, NA., Fass, JN. Sickle: A sliding-window, adaptive, quality-based trimming tool for FastQ files. 2011. (available at https://github.com/najoshi/sickle)
37. Benson DA, et al. GenBank. Nucleic Acids Research. 2013; 41:D36–42. [PubMed: 23193287]
38. Langmead B, Salzberg SL. Fast gapped-read alignment with Bowtie 2. Nat Chem Biol. 2012; 9:357–359.
39. DePristo MA, et al. A framework for variation discovery and genotyping using next-generation DNA sequencing data. Nat Genet. 2011; 43:491–498. [PubMed: 21478889]

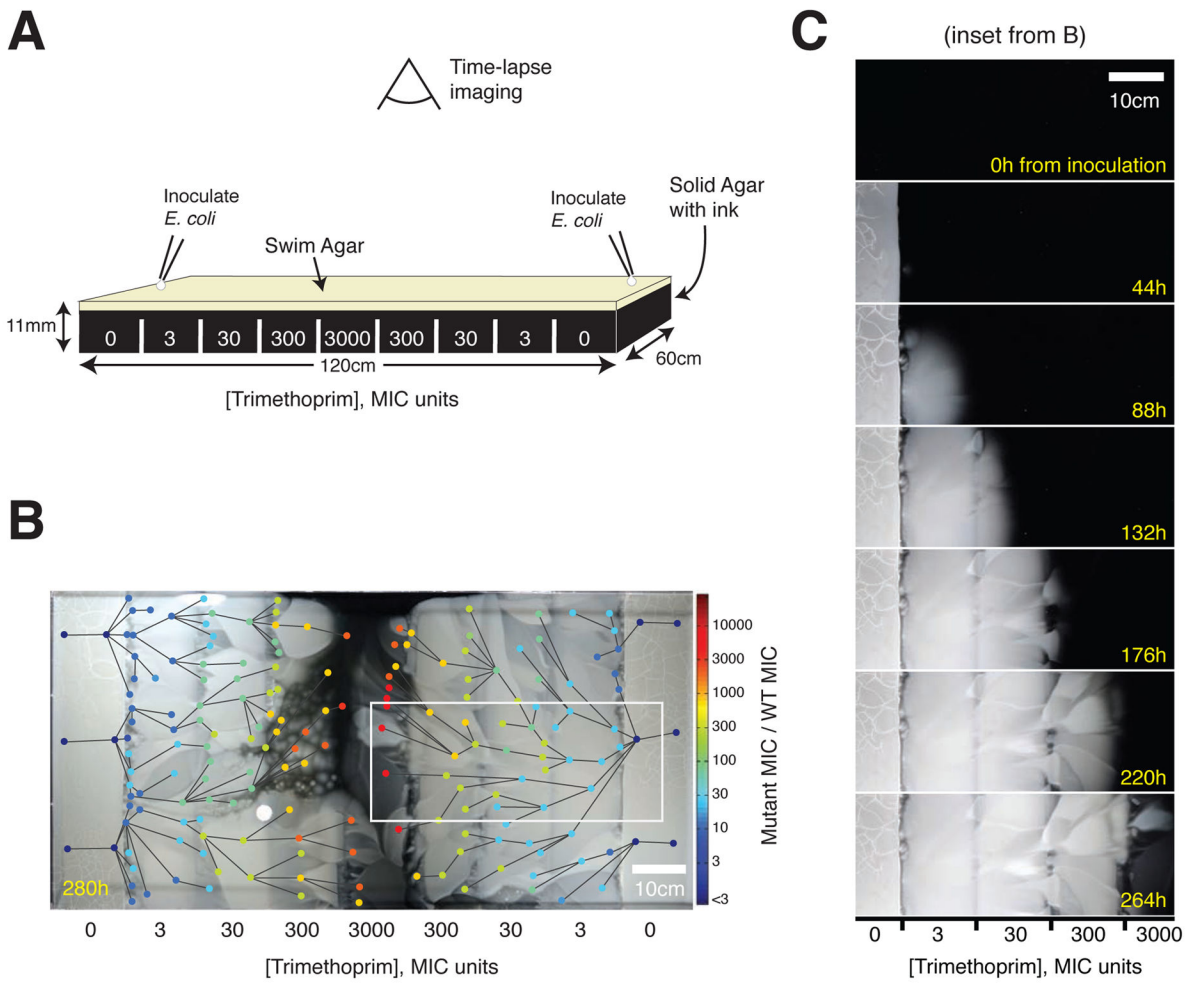

Fig. 1. An experimental device for studying microbial evolution in a spatially structured environment

(**A**) Setup of the four-step gradient of Trimethoprim (TMP). Antibiotic is added in sections to make an exponential gradient rising inwards. (**B**) The four-step TMP MEGA-plate after 12 days. *E. coli* appear as white on the black background. The 182 sampled points of clones are indicated by circles, colored by their measured MIC. Lines indicate video-imputed ancestry. (**C**) Time-lapse images of a section of the MEGA-plate. Repeated mutation and selection can be seen at each step. Images have been aligned and linearly contrast-enhanced but are otherwise unedited.

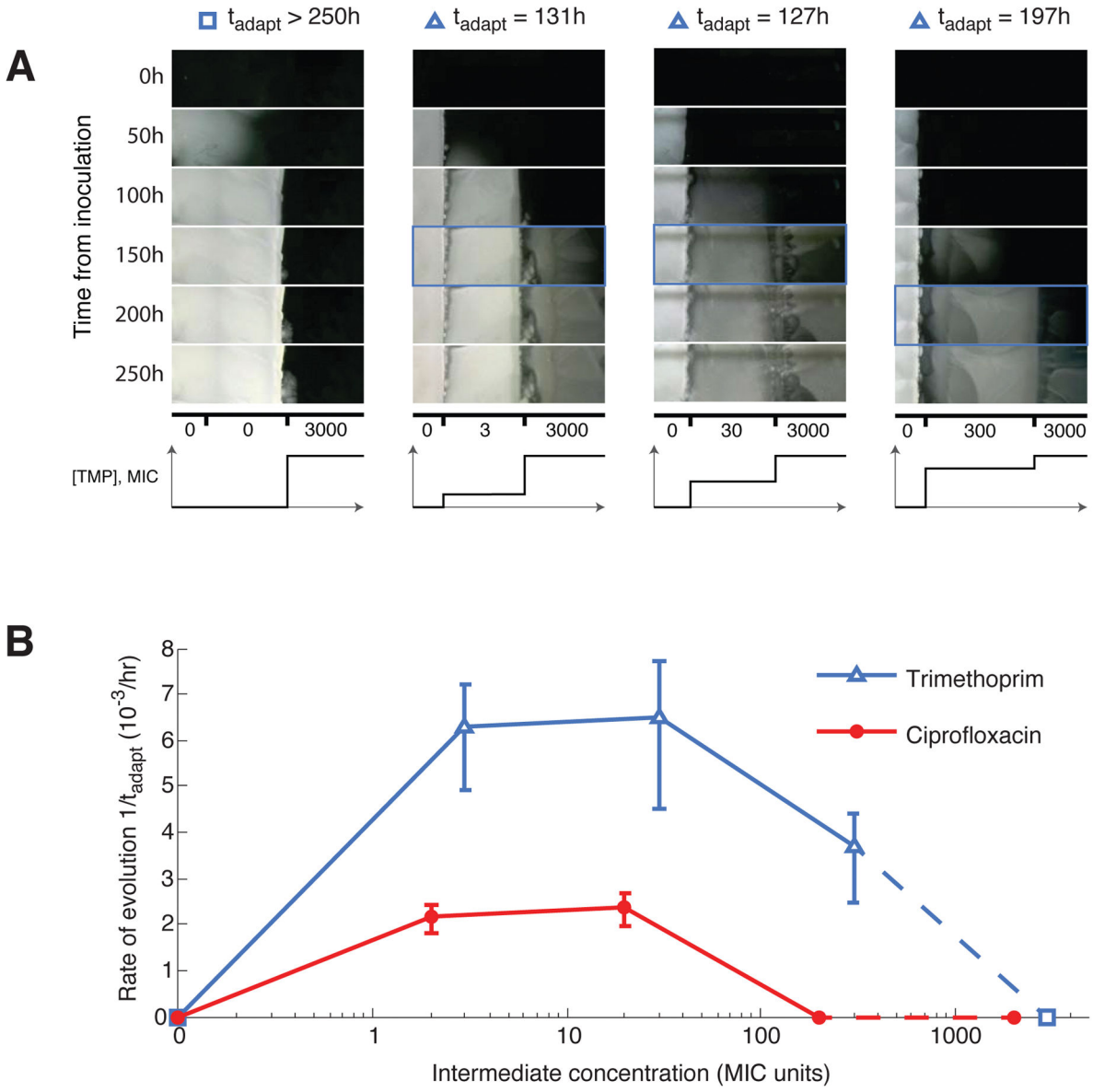

Fig. 2. Initial adaptation to low drug concentrations facilitates later adaptation to high concentrations

(**A**) Frames from a section of the TMP intermediate step MEGA-plate over time (TMP, movie S4; CPR, movie S5). The first frame showing a mutant in the highest band is indicated by a blue box. (**B**) The rates of adaptation in the intermediate step experiments across TMP and CPR, showing the necessity of intermediate adaptation for the evolution of high levels of resistance. Error bars show the appearance times of multiple lineages in the highest concentration. As the intermediate step with no drug puts the highest and lowest concentrations adjacent, it serves as both the highest and lowest intermediate steps (dotted line).

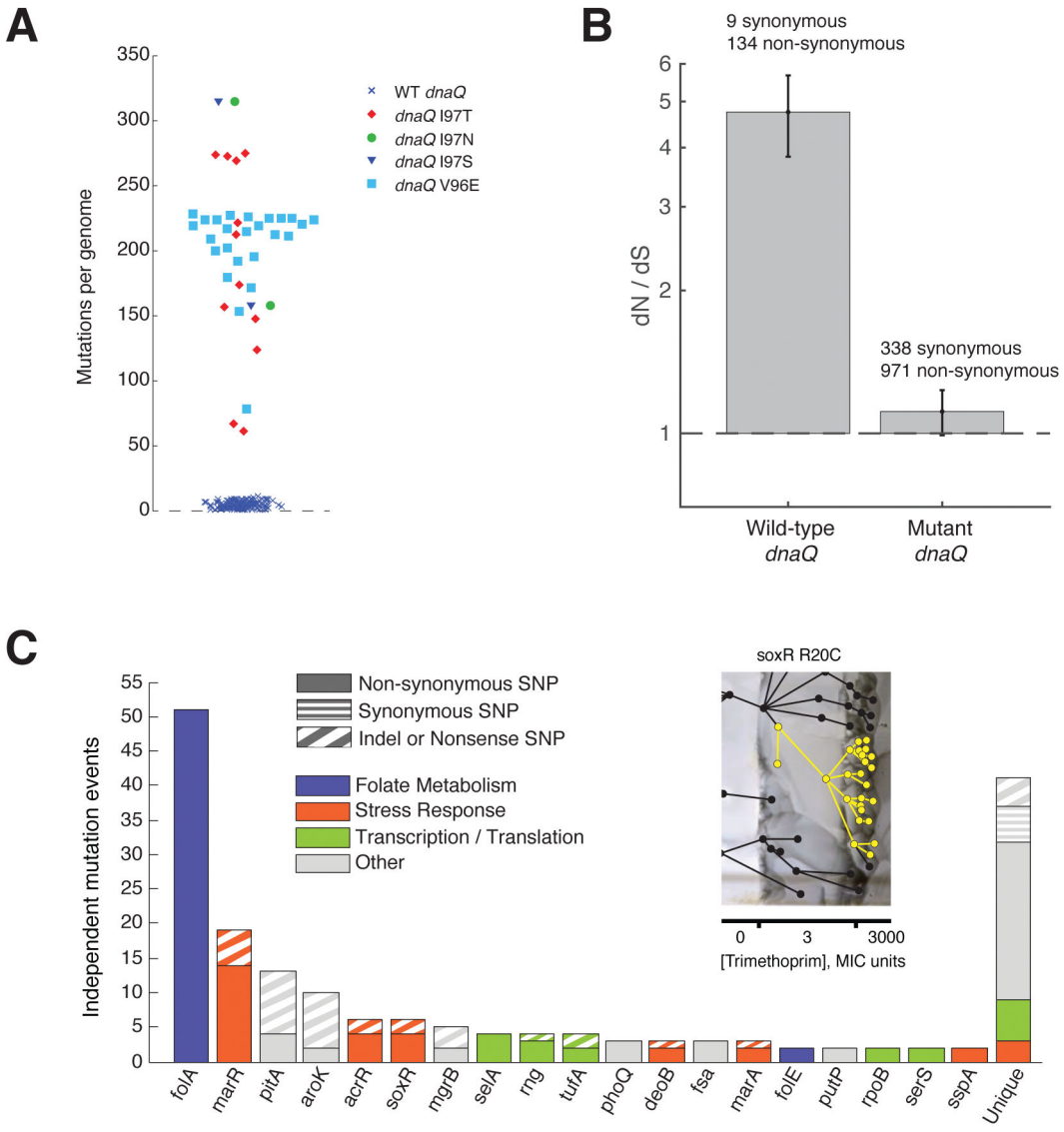

Fig. 3. Diverse genotypic strategies for adaptation to trimethoprim

(**A**) The number of observed mutations across individual isolates. Samples with a *dnaQ* mutation (filled symbols) consistently carried more mutations than those sampled with the wild-type *dnaQ* allele ('x' symbols). Data points are horizontally jittered for clarity. (**B**) The normalized ratio of non-synonymous to synonymous substitutions of isolates compared with the ancestor for samples with normal and highly mutated phenotypes. Error bars are the standard deviation of the Bayesian posterior estimate for the binomial parameter. **(C)** The number of distinct mutational events in genes that were mutated at least twice independently. Genes are colored by pathway per EcoCyc (33). Non-synonymous, synonymous and loss of function (including indel and nonsense) are indicated by the fill. Genes that only had one mutation across all samples were combined into the "unique" column. Individual mutations events were inferred through ancestry (movies S1 and S4). Inset: The multi-step MEGA-plate with samples containing the mutation *soxR* R20C (yellow) tracing mutational events from multiple samples and video.

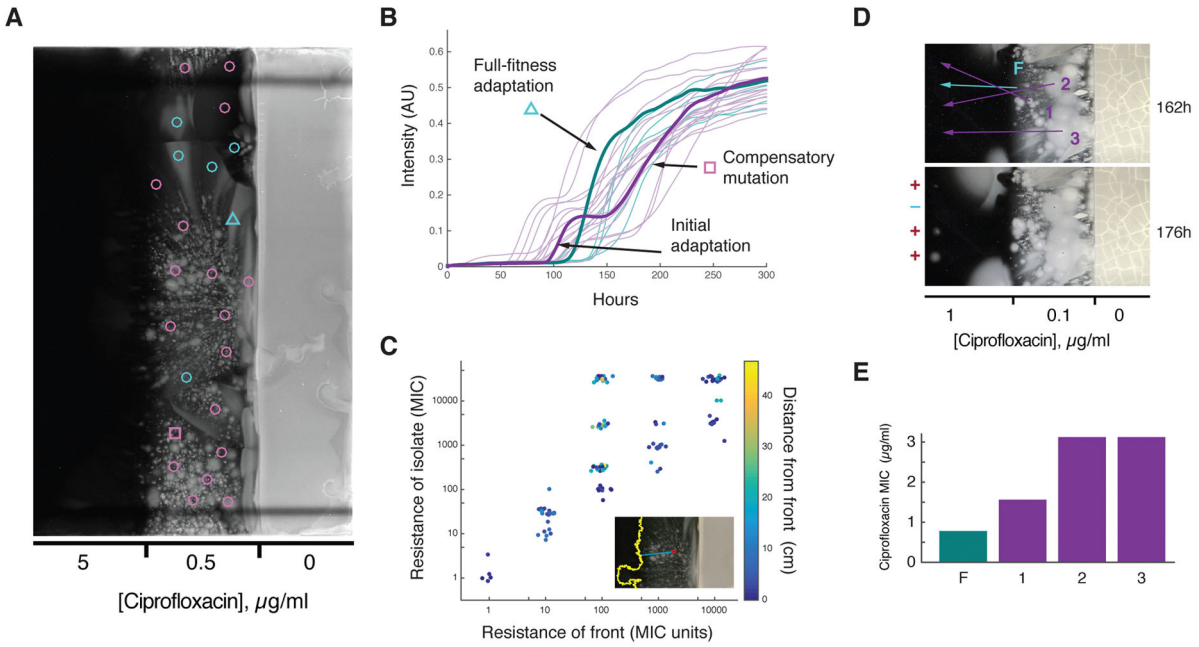

Fig. 4. Compensatory mutations can be spatially trapped

(A) Ciprofloxacin experiment still frame with locations of 24 isolates showing a full-fitness mutation (cyan) or yield-deficient mutation followed by a compensatory mutation (purple). **(B)** Optical density at the marked points in (A) over the course of the experiment. The two example traces (indicated by a square and triangle) correspond to the points marked by the same glyph in (A). **(C)** Mutants isolated behind the front can have significantly higher resistance than the front at the time it passed the same location. Resistance of the front was measured by the concentration at which front progression stopped, isolate MICs were measured *in vitro*. **(D)** The front (marked F), and three compensatory mutants (marked 1–3), were sampled at 162 hours, and immediately inoculated ahead of the front as indicated by the arrows. Growth of the moved mutants is evident for the three compensatory mutants, despite being inoculated at a CPR concentration dramatically higher than where they emerged, but not for the front. **(E)** Measured CPR MICs of the mutants from (D).